Issues in the comparison of particle perturbations and numerical relativity for binary black hole mergers

Richard H. Price◉

Department of Physics, MIT, 77 Massachusetts Avenue, Cambridge, Massachusetts 02139, USA

Gaurav Khanna

Department of Physics, East Hall, University of Rhode Island, Kingston, Rhode Island 02881, USA
and Department of Physics and Center for Scientific Computing and Data Research,
University of Massachusetts, Dartmouth, Massachusetts 02747, USA

Recent work on improved efficiency of calculations for extreme mass ratio inspirals has produced the useful byproduct of comparisons of inspirals of comparable mass by particle perturbation (PP) methods and by numerical relativty (NR). Here we point out: (1) In choosing the rescaling of the masses, consideration must be given to the differences in the PP and NR methods even in the earliest, least nonlinear regime—in particular barycenter effects must be addressed; (2) Care must be given to the comparison of the nonspinning remnant in PP and the rapidly spinning remnant in NR.

I. INTRODUCTION

Next generation interferometric gravitational wave (GW) detectors will be sensitive to signals from inter-mediate/extreme mass-ratio inspirals (I/EMRIs) of binary black holes. For such sources a numerical relativity (NR) solution of the full nonlinear Einstein equations may prove to be challenging and may not be needed. Other modeling methods for I/EMRIs include point-particle black hole perturbation theory [1,2], the gravitational self-force [3–8] and effective-one-body (EOB) [9–15]. High accuracy and improved insights are likely to come from particle perturbation (PP) methods. Even these methods, however, are computationally expensive. To reduce the computational cost of NR and I/EMRI calculations, data-driven "surrogate" models have been developed [16–18]. Machine learning based surrogate models presented in Refs. [17,18] are "trained" using PP waveforms calibrated with NR results for various values of the ratio q of M_1, the more massive hole, to the smaller hole M_2.

Every method is limited in the value of $q \equiv M_1/M_2$ for which it is appropriate. For q much greater than approximately 10, NR cannot easily handle the great disparity in grid size around the two black hole regions. PP on the other hand, treats M_2 as a perturbation on the spacetime of M_1. It is therefore appropriate for the EMRI limit and may yield astrophysically reasonable results for q much greater than around 10. But, despite low expectations of accuracy, there is nothing that prevents PP codes from running for smaller values

of q, i.e., for comparable mass holes, and from comparing the results to those of NR. It has been somewhat surprising that the results of these PP explorations, when simply rescaled, agree rather well with the NR results [17,18].

Because black hole processes scale in black hole mass, confusion lurks as a possibility in interpreting both NR and PP data. The numbers reported in both cases, what might be called "raw" data, have to be multiplied by a mass to produce dimensional data. The relevant dimensional data in both cases are the periods of the GW oscillations and the product of the (dimensionless) GW strain h with the (dimensional) radius r at which the GW data are extracted.

A correct interpretation of conversion from raw to dimensional numbers is that in the NR case, the raw numbers are to be multiplied by the total mass of the spacetime $M_{\text{total}} = M_1 + M_2$, while the PP results are to be multiplied by the larger mass M_1.

If we want to compare physically equivalent configurations being computed in the two methods, then we must arrange for them to refer to the same value of M_1. If we were to compare the "raw" data we would be comparing PP and NR data for different M_1. To correct for this, the raw data for PP must be reduced to a scaling corresponding to the M_1 of the NR computations. This means reducing the PP raw data by a factor $M_1/M_{\text{total}} = 1/(1 + 1/q)$ This is what was done in the surrogate papers, and what we, like those authors, will call the naive rescaling.
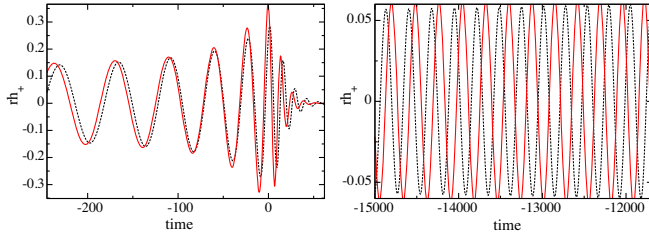
FIG. 1. Comparison of NR results (dashed-black curve) for gravitational wave amplitude, and "naively" rescaled PP results (solid-red curve) for $q = 3$. The rescaling is a reduction of both the time and the gravitational wave strength rh_+ by the factor of $1/(1 + 1/q) = 0.75$. The curves are aligned so that the peaks of both the NR and PP runs agree.

For our primary example, $q = 3$, this naive reduction factor is 0.75. We compared the NR[1] [19] and PP raw data [1] for $q = 3$ from very early Newtonian orbits, with a separation on the order of $3GM_{\text{total}}/c^2$, to very late quasinormal ringing—for the entire range of cycles we find a NR/PP ratio of gravitational wave periods 0.79 ± 0.2.

For $q = 3$ we show the result of naive scaling in Fig. 1. The dashed-black curves are the NR results. The solid red curves are the PP results rescaled with reduction of values on both axes by the naive scaling $1/(1 + 1/q) = 0.75$. The curves are aligned so that the peaks of both the NR and PP runs agree. It is clearly seen that although the amplitudes are in rough agreement, the phases are not.

The purpose of this paper is to discuss the considerations for a proper NR/PP comparison. This is a needed first step if the physics of nonlinearities (beyond the *adiabatic* radiative corrections) is to be extracted from the comparison.

The considerations will be presented in three separate sections: The problem of aligning waveforms in Sec. II; The inclusion of barycenter effects in Sec. III; the comparison of quasinormal ringing and considerations of the spin of the remnant, in Sec. IV; and comments on the relation of our results with those from optimization [18] in Sec. V. Some mention of possible future directions is given in Sec. VI.

II. OVERALL ALIGNMENT

The gravitational waveforms from NR and PP are a list of raw times and the corresponding raw values for the gravitational wave amplitudes rh_+.[2] Since some rescaling,

FIG. 2. Aligned rescaled data for $q = 3$. NR data is the solid-red curve and the rescaled PP is depicted by the dashed-black one. Rescaling is done by reducing both the period and GW amplitude by the "naive" scaling factor $(1 + 1/q)$, due to the different total masses in NR and PP results for the same M_1. The PP periods are then decreased by an additional factor $(1 + 1/q)^{1/2}$ due to barycenter effects (explained in Sec. III) that have been omitted from previous PP work. Axis are in units of M_{total}.

whether naive or sophisticated, will be needed, it should be clear that simply comparing the waveforms at equivalent raw times does not amount to comparison at equivalent physical configurations. (The small range 0.79 ± 0.2 of the NR/PP period ratio, therefore, offers little physical insight.) Previous attempts to compute the rescaling via an optimization procedure [17,18] while it led to an unexpected agreement with NR, were also not physically well motivated.

What then is the right way to make the comparison? For the earliest GW cycles the orbits creating the waveforms are very nearly Keplerian. Subsequent differences between the PP and NR waveforms can then be understood as signs of nonlinear effects beyond the adiabatic radiative correction. Figure 2 shows the results when this is done with the $q = 3$ data for NR and PP. This alignment requires the use of the rescaling, explained in the next section. This is completely "theoretical" rescaling based on Keplerian orbits, with no optimization. When the theoretical rescaling is applied to the GW periods in the PP data, the NR waveforms are searched for the same period. In the case illustrated in Fig. 2, the earliest period used in the PP data was around the raw time of -28000, and the raw period[3] is approximately 430. The corresponding theoretically rescaled period is 280. A search was then made in the NR data for this period, and was found at time around -15000. The rescaled PP data was then moved so that the GW oscillations overlap. *The agreement of the rescaled GW amplitude in the PP data and the GW amplitude in the NR data confirms the validity of the procedure.*

---

[1]It should be noted that NR cannot produce long wave trains, therefore we use a hybridized surrogate model that combines late stage NR data with the EOB model to generate long-duration inspiral waveforms. We will refer to the hybrid models simply as NR, since the issues we discuss (alignment, barycenter, QNR) apply in the same way to the hybrid results as to NR results.

[2]We have found nothing different about what can be extracted from $h_\times$, the other polarization, so for simplicity we limit discussion to h_+.

[3]Found by subtracting the raw times between two consecutive peaks or troughs.

While some effort was made in order to test the robustness of this procedure, it should be noted that for very long waveforms that involve many inspiral cycles with very slowly varying periods, it may be difficult in practice to perform an alignment robustly based on the approach taken above.

III. EARLY CYCLES: BARYCENTER

In the early cycles both NR and PP computations have negligible nonlinear effects, but they are not based on the same models. In particular, PP treats the binary dynamics as if the coordinate origin, the center of M_1, were an inertial point. This of course is not physically correct. It is the barycenter of the two black holes that is the inertial point. With R_1, R_2 representing, respectively, the distance from the barycenter to M_1, M_2 a very straightforward calculation gives the angular velocity about the barycenter to be

$$\Omega_{\text{bar}} = \sqrt{\frac{M_1}{R_2 s^2}}, \tag{1}$$

where $s \equiv R_1 + R_2$. For the PP analysis the angular velocity around the coordinate origin is

$$\Omega_{\text{PP}} = \sqrt{\frac{M_1}{s^3}}. \tag{2}$$

From these we find that the ratio of the period about the barycenter to that about M_1 is

$$\frac{T_{\text{bar}}}{T_{\text{PP}}} = \sqrt{\frac{R_2}{s}} = \sqrt{\frac{1}{1 + 1/q}}. \tag{3}$$

The overall rescaling of the PP period is then $(1 + 1/q)^{-3/2}$, consisting of a decrease by a factor $(1 + 1/q)$, due to the change of units and an decrease by $(1 + 1/q)^{1/2}$ from the barycenter omission of the PP method.

We need to ask next how the barycenter omission affects the GW amplitude in the PP work. To do this we use the "slow motion" approximation [23] and compute the ratio of ℓ-pole moments in the PP and NR approaches,

$$\frac{Q_{\text{bar}}^\ell}{Q_{\text{PP}}^\ell} = \frac{M_1 R_1^\ell + M_2 R_2^\ell}{M_2 s^\ell} = \frac{1 + 1/q^{\ell-1}}{(1 + 1/q)^\ell}. \tag{4}$$

The GW amplitude in the ℓth moment is proportional to the ℓth time derivative of Q^ℓ so, with Eq. (3), we have

$$\frac{h_{\text{bar}}^\ell}{h_{\text{PP}}^\ell} = \frac{1 + 1/q^{\ell-1}}{(1 + 1/q)^{\ell/2}}, \tag{5}$$

and the interesting conclusion is that for *the dominant quadrupole radiation the GW amplitude is not affected by*

the omission of barycenter effects in the PP computation. The gravitational wave amplitude must only be scaled by the naive unit scaling. This has been done in Fig. 2; *the PP period has been divided by* $(1 + 1/q)^{3/2}$ *and the amplitude has been reduced by* $(1 + 1/q)$.

It is natural to ask how the agreement shown in Fig. 2 compares with the agreement for naive scaling. That is, how does the NR waveform compare to the PP waveform if the alignment is adjusted for a best fit to the period? The brief answer is that the fit is about equally good at least in one sense; in both cases the NR and PP waveforms drift 180° out of phase after around 35 GW periods.

A more careful answer involves several considerations. Most important, over the ≈35 periods of alignment drift, both the NR and PP periods change by around 23%. This is a much larger drift of phase than what is observed in the NR vs PP comparison.

The comparison of "fit" then is not a good basis for a quick evaluation of the naive vs improved scaling. What is a good basis is a comparison of amplitudes for the best fits? As shown in Fig. 2, a best fit to the period, gives excellent agreement with the amplitude. By comparison, for a best fit in the naive case, the PP amplitude is larger by 10.7% than the NR amplitude.

Underlying the match in Fig. 2 is the assumption that Keplerian orbits describe the motions in both the PP and NR work, and linearized general relativity is adequate for the GW amplitude. It is interesting therefore to note that the simple quadrupole formula [29] underestimates the GW amplitude by around 10%—much larger than would be suspected from Fig. 2. It should also be noted that for $\ell = 3$, the rescaling implied by Eq. (5), along with the naive rescaling, implies a reduction of the PP raw data by a factor of 0.54, whereas the raw data, when aligned, shows a ratio of around 0.41.

IV. LATE CYCLES: QUASINORMAL RINGING

At the end of both the NR and PP waveforms there is the characteristically strongly damped, high-frequency oscillations of quasinormal ringing (QNR). It is noted in Ref. [17] that a rescaling close to the naive rescaling brings the QNR of the PP waveform into agreement with the QNR of the NR waveform. That is an intriguing result, especially if one appreciates that the remnant in the NR work is a rotating Kerr hole, while the PP calculation maintains the Schwarzschild form it started with. To underscore this, Table I shows that this kind of rescaling works well only for $q \gtrsim 5$ and for these values we view the agreement to be simply due to the fact that the there is little variation for $5 < q < \infty$ and the remnant QN oscillation frequency is expected to increase with decreasing q [30].

Although this particular aspect of the PP/NR comparison is not very useful, it turns out that a PP-related calculation gives a remarkably accurate estimate of the remnant spin. The underlying principle [24–26] is that negligible angular

TABLE I.   Comparison of the QNR frequency for a remnant and the rescaled Schwarzschild QNR frequency. For each value of q in the first column, the second column gives the remnant value of the spin parameter a listed in the SXS catalog [21] for the SXS model, given in the third column, a model with negligible initial spins. The fourth column gives the real part of the least damped $\ell, m = 2, 2$ quasinormal frequency, from the tables in Ref. [30]. The last column gives the frequency for $a = 0$ with "naive" rescaling. We do not show the QNR damping times because extracting those values accurately is difficult and they do not vary much for the moderate range in a that we are considering here.

q	SXS $\chi_{\rm rem}$	SXS ID	$\omega_{\rm R}^{\rm Kerr}$	$(1 + 1/q)\,\omega_{\rm R}^{rmSchw}$
1.5	0.6641	BBH:007	0.5175	0.6228
2	0.6234	BBH:0169	0.5021	0.5605
2.5	0.5807	BBH:0259	0.4877	0.5231
3	0.5406	BBH:0030	0.4755	0.4982
4	0.4716	BBH:0182	0.4567	0.4671
5	0.4166	BBH:0054	0.4436	0.4484
6	0.3725	BBH:0181	0.4438	0.4360
8	0.3067	BBH:0063	0.4208	0.4204
9.5	0.2708	BBH:0302	0.4142	0.4130
∞	0	–	0.37367	0.37367

momentum is radiated after the binary enters the plunge. For a merger of nonspinning holes, therefore, the angular momentum of the remnant should be the orbital angular momentum of the binary at the innermost stable circular orbit.

The predicted spin of the remnant is given in Refs. [24–26] but, for completeness, are repeated here for a particle of mass μ, in a circular orbit of radius r, around a Kerr hole of parameters M, a. From Ref. [22] the angular momentum L_z is found

$$\frac{L_z}{\mu} = \frac{M^{1/2}(r^2 - 2a\sqrt{Mr} + a^2)}{r^{3/4}\sqrt{r^{3/2} - 3Mr^{1/2} + 2aM^{1/2}}} \quad (6)$$

and the radius of the innermost stable circular orbit is given by

$$Z_1 = 1 + \left(1 - \frac{a^2}{M^2}\right)^{1/3}\left[\left(1 + \frac{a}{M}\right)^{1/3} + \left(1 - \frac{a}{M}\right)^{1/3}\right], \quad (7)$$

$$Z_2 = \sqrt{3a^2/M^2 + Z_1^2}, \quad (8)$$

$$r_{\rm ISCO} = M[3 + Z_2 - {\rm sgn}\,a\sqrt{(3 - Z_1)(3 + Z_1 + 2Z_2)}]. \quad (9)$$

In Eqs. (6)–(9), M is the total spacetime mass. We use the notation $[L_z/\mu]$ to mean the expressions above with $M = 1$. In our notation the expression $[L_z/\mu]$ is dimensionless and has the meaning

$$\left[\frac{L_z}{\mu}\right] \equiv \frac{\text{angular momentum}}{(\text{particle mass})(M_1 + M_2)}. \quad (10)$$

We take the particle mass to be the reduced mass of the system,

$$\mu \equiv \text{particle mass} = \text{reduced mass} = \frac{M_1 M_2}{M_1 + M_2}. \quad (11)$$

In our comparisions we will be using the dimensionless spin $\chi_{\rm rem}$ of the remnant defined in the SXS catalog as L_z divided by the square of the total system mass. The comparable quantity in our PP work is the dimensionless spin

$$\begin{aligned} a_{PP} &= \frac{L_z}{(M_1 + M_2)^2} = \left[\frac{L_z}{\mu}\right]\frac{\text{particle mass}}{(M_1 + M_2)} \\ &= \left[\frac{L_z}{\mu}\right]\frac{M_1 M_2}{(M_1 + M_2)^2} \\ &= \left[\frac{L_z}{\mu}\right]\frac{q}{(1 + q)^2}. \end{aligned} \quad (12)$$

In our table below we find this value for given system parameters by computing $[L_z/\mu]$ from Eqs. (6)–(9), with $M = 1$, and a moderate, but arbitrary, choice for a. The resulting a_{PP} is then used as the starting point in Eqs. (6)–(9), and the procedure is iterated until a stable PP "prediction" is found for a_{PP}. This result is then compared with the value of $\chi_{\rm rem}$ for the same model.

The accuracy of this approximation can be seen in the comparison with the NR results in the SXS catalog. *The excellent agreement of this approximation with NR results supports the argument [24–26] that little angular momentum is radiated during the plunge and merger.*

TABLE II.   Comparison of the Kerr spin parameter for a remnant from NR and PP. For each value of q in the first column, the second column gives the remnant value of the spin parameter a listed in the SXS catalog [21] for an SXS model, given in the third column, with negligible initial spins. The last column gives the comparable spin parameter computed by the procedure described in Eqs. (6)–(12), and show excellent agreement.

q	SXS $\chi_{\rm rem}$	SXS ID	a_{PP}
1.5	0.6641	BBH:007	0.6442
2	0.6234	BBH:0169	0.6092
2.5	0.5807	BBH:0259	0.5714
3	0.5406	BBH:0030	0.5350
4	0.4716	BBH:0182	0.4708
5	0.4166	BBH:0054	0.4182
6	0.3725	BBH:0181	0.3753
8	0.3067	BBH:0063	0.3103
9.5	0.2708	BBH:0302	0.2742
∞	0	–	0.0

It is interesting to consider how the accuracy of our PP approximation is modified if the holes have nonzero initial spin. As an example, we consider the SXS model BBH:0051, with $q = 3$, with an initially nonspinning smaller hole, but $\chi_1 = Lz/(M_1)^2 = 0.5$ for the more massive black hole. We use our procedure in Eqs. (6)–(9). We add the contribution to a_{PP} due to the angular momentum carried by M_1, which means adding $\chi_1 M_1^2/(M_1 + M_2)^2$. We then use the result as the input for the next iteration. The result, the PP prediction, is 0.7056, in rough agreement with the SXS result 0.7551. For SXS model BH:0049, it is the smaller hole that is spinning, with $\chi_2 = 0.5$. In this case, our PP procedure predicts $a_{PP} = 0.6217$, in rough agreement with the comparable SXS value 0.5773.

Reference [26] gives an extensive exploration of parameter space for the remnant spin approximation. Both in that reference and in our two examples above, the accuracy of the simple model is worse when there is initial spin rather than no spin. This suggests that tidal interaction during the pre-ISCO motion may play a non-negligible role.

V. COMPARISON WITH OPTIMAL RESCALING OF REFERENCE [18]

In Ref. [18] an optimization procedure was used to compute the rescaling parameters for PP in order to maximize agreement with NR. In particular, the PP amplitude was scaled by a parameter α and the time (period) by β. Then α and β were computed in order to minimize the L^2-norm difference between the rescaled PP and NR waveforms. As an example, for $q = 3$ and for the h_{22} waveform the optimal values of α and β were both found to be 0.7 approximately. The α and β values based on the total mass and barycenter corrections we present here are $\alpha = 0.75$ and $\beta = 0.65$. While we do not view a direct comparison of these values as meaningful, but the fact that the optimized rescaling yields good agreement with NR over the entire waveform duration does suggest that there are other (nonlinear) corrections that are somehow being addressed through the optimized rescaling procedure over the barycenter correction that we have identified here.

In the context of higher modes, it has been noted that the value of β stays the same as the dominant $\ell = m = 2$ case, but the value of the amplitude rescaling α drops significantly [18]. For example, for $\ell = m = 3$ the optimal value of $\alpha = 0.4$, a sharp drop from 0.7 for the $\ell = m = 2$ case. It has been suggested that the drop in the amplitude rescaling comes from the fact that the PP calculation does not account for the substantial size of the smaller black hole in the context of comparable mass ratios like $q = 3$ [18]. In other words, the PP approximation generates artificially higher amplitudes for higher modes due to the fact that the PP itself has a wider bandwidth than an object of finite size. We argue that while this issue is likely to play a role, it

should only be significant for much larger values of ℓ, m because the wavelength of the radiation would need to become comparable to the size of the smaller black hole [31]. Instead, as we pointed out in Sec. III the barycenter corrections we propose here result in a value of $\alpha = 0.54$ which is strongly suggestive of a large drop from the value of 0.75 computed for the $\ell = m = 2$ case.

VI. CONCLUSIONS

As stated in the Introduction section, the comparison of PP results and NR results are a resource for probing the interaction of inspiraling black holes as they draw closer. Exploiting this, however, must be done in a way that compares the two methods at physically equivalent moments of the inspiral. We have pointed out that this has not been done in the work associated with establishing surrogate models [17,18]. The goal of that effort was to use NR results as calibration data for high-mass ratio gravitational waveform computations. We suggest that such models may be aided by addressing the issues we raise above about alignment and physically based rescaling.

Aside from that, possible directions should be considered for future work. The loss of spin angular momentum during inspiral, and its connection to tidal interactions, has already been made in Sec. IV. Work has already been started in this area [26]. We have also pointed out in Sec. III, that the quadrupole formula and the equivalent for the octupole are less accurate than might be expected. These formulas are slow-motion approximations and are being applied in what would appear to be an appropriate setting. Understanding why the formulas miss the mark may be very useful in a variety of applications.

As a much more challenging extension of the PP/NR comparison, one might consider binary inspirals of holes with spin angular momentum not aligned with orbital angular momentum. Such a comparison would be helpful in understanding how to use a spinning particle as a proxy for a rotating black hole.

We also expect that there are other insights that can be extracted from an extended PP/NR comparison; insights beyond our current imagination.

[1] Pranesh A. Sundararajan, Gaurav Khanna, and Scott A. Hughes, Phys. Rev. D **81,** 104009 (2010); Anil Zenginoglu and Gaurav Khanna, Phys. Rev. X **1,** 021017 (2011); Justin McKennon, Gary Forrester, and Gaurav Khanna, *Proceedings of the NSF XSEDE12 Conference, Chicago* (Association for Computing Machinery, Chicago, Illinois, 2012), 10.1145/2335755.2335808; Scott E. Field, Sigal Gottlieb, Zachary J. Grant, Leah F. Isherwood, and Gaurav Khanna, Commun. Appl. Math. Comput. Sci. (2021).10.1007/s42967-021-00129-2.

[2] Enno Harms, Sebastiano Bernuzzi, Alessandro Nagar, and Anil Zenginoglu, Classical Quantum Gravity **31,** 245004 (2014).

[3] Adam Pound, Motion of small objects in curved spacetimes: An introduction to gravitational self-force, in *Equations of Motion in Relativistic Gravity*, Fundamental Theories of Physics, edited by D. Puetzfeld, C. Laemmerzahl, and B. Schutz (Springer, Cham, 2015), Vol. 179.

[4] Adam Pound, Phys. Rev. D **95,** 104056 (2017).

[5] Leor Barack and Adam Pound, Rep. Prog. Phys. **82,** 016904 (2019).

[6] Barry Wardell, Adam Pound, Niels Warburton, Jeremy Miller, Leanne Durkan, and Alexandre Le Tiec, arXiv:2112.12265.

[7] Adam Pound, Barry Wardell, Niels Warburton, and Jeremy Miller, Phys. Rev. Lett. **124,** 021101 (2020).

[8] Niels Warburton, Adam Pound, Barry Wardell, Jeremy Miller, and Leanne Durkan, Phys. Rev. Lett. **127,** 151102 (2021).

[9] Alessandra Buonanno and Thibault Damour, Phys. Rev. D **59,** 084006 (1999).

[10] Alessandra Buonanno and Thibault Damour, Phys. Rev. D **62,** 064015 (2000).

[11] Thibault Damour, Piotr Jaranowski, and Gerhard Schaefer, Phys. Rev. D **62,** 084011 (2000).

[12] Thibault Damour, Phys. Rev. D **64,** 124013 (2001).

[13] Thibault Damour, Piotr Jaranowski, and Gerhard Schaefer, Phys. Rev. D **91,** 084024 (2015).

[14] Alessandro Nagar, James Healy, Carlos O. Lousto, Sebastiano Bernuzzi, and Angelica Albertini, Phys. Rev. D **105,** 124061 (2022).

[15] Angelica Albertini, Alessandro Nagar, Adam Pound, Niels Warburton, Barry Wardell, Leanne Durkan, and Jeremy Miller, arXiv:2208.01049 [Phys. Rev. D (to be published)].

[16] Vijay Varma, Scott E. Field, Mark A. Scheel, Jonathan Blackman, Davide Gerosa, Leo C. Stein, and Lawrence E. Kidder, Phys. Rev. Res. **1,** 033015 (2019).

[17] Nur E. M. Rifat, Scott E. Field, Gaurav Khanna, and Vijay Varma, Phys. Rev. D **101,** 081502 (2020).

[18] Tousif Islam, Scott E. Field, Scott A. Hughes, Gaurav Khanna, Vijay Varma, Matthew Giesler, Mark A. Scheel, Lawrence E. Kidder, and Harald P. Pfeiffer, arXiv:2204.01972.

[19] Vijay Varma, Scott E. Field, Mark A. Scheel, Jonathan Blackman, Lawrence E. Kidder, and Harald P. Pfeiffer, Phys. Rev. D **99,** 064045 (2019).

[20] Michael Boyle *et al.*, Classical Quantum Gravity **36,** 195006 (2019); Abdul Mrue *et al.*, Phys. Rev. Lett. **111,** 241104 (2013).

[21] SXS Collaboration, SXS Waveform Catalog, https://data.black-holes.org/waveforms/catalog.html.

[22] James M. Bardeen, William H. Press, and Saul A. Teukolsky, Astrophys. J. **178,** 347 (1972).

[23] Kip S. Thorne, Rev. Mod. Phys. **52,** 299 (1980).

[24] Scott A. Hughes and Robert D. Blandford, Astrophys. J. **585,** L101 (2003).

[25] Kostas Glampedakis, Scott A. Hughes, and Daniel Kennefick, Phys. Rev. D **66,** 064005 (2002).

[26] Alessandra Buonanno, Larry Kidder, and Luis Lehner, Phys. Rev. D **77,** 026004 (2008).

[27] Stephen Detweiler and Eric Poisson, Phys. Rev. D **69,** 084019 (2004).

[28] Emanuele Berti, Vitor Cardoso, and Andrei O. Starinets, Classical Quantum Gravity **26,** 163001 (2009).

[29] Charles W. Misner, Kip S. Thorne, and John A. Wheeler, *Gravitation* (W. H. Freeman, San Francisco, 1973), Eq. 36.20.

[30] Emanuele Berti, Ringdown Data, https://pages.jh.edu/eberti2/ringdown/.

[31] Enrico Barausse, Emanuele Berti, Vitor Cardoso, Scott A. Hughes, and Gaurav Khanna, Phys. Rev. D **104,** 064031 (2021).